

AutoSF+: Towards Automatic Scoring Function Design for Knowledge Graph Embedding

Yongqi Zhang

zhangyongqi@4paradigm.com

4Paradigm Inc.

Beijing, China

Zhanke Zhou

zhouhanke@4paradigm.com

4Paradigm Inc.

Beijing, China

Quanming Yao

qyaoaa@tsinghua.edu.cn

Tsinghua University & 4Paradigm Inc.

Beijing, China

ABSTRACT

Scoring functions, which measure the plausibility of triples, have become the crux of knowledge graph embedding (KGE). Plenty of scoring functions, targeting at capturing different kinds of relations in KGs, have been designed by experts in recent years. However, as relations can exhibit intricate patterns that are hard to infer before training, none of them can consistently perform the best on existing benchmark tasks. AutoSF has shown the significance of using automated machine learning (AutoML) to design KG-dependent scoring functions. In this paper, we propose AutoSF+ as an extension of AutoSF. First, we improve the search algorithm with the evolutionary search, which can better explore the search space. Second, we evaluate AutoSF+ on the recently developed benchmark OGB. Besides, we apply AutoSF+ to the new task, i.e., entity classification, to show that it can improve the task beyond KG completion.

KEYWORDS

Automated machine learning, Knowledge graph embedding

1 INTRODUCTION

Knowledge Graph (KG) [36, 45, 51] is a special kind of graph data in which the nodes represent entities and edges are the relations between entities. KG plays vital roles in areas of data mining and machine learning, boosting various downstream applications such as question answering [34, 42] and recommendation [30]. Extensive studies have been done on knowledge graph embedding (KGE), which learns a mapping from the symbolic entities and relations to low-dimensional embedding vectors that best preserve the semantical and topological properties in the original KGs [25, 51].

One should attach attention to encoding the interactions of entities and relations to obtain high-quality representations of KG. A general method is to define a scoring function (SF) to capture such interactions. The SF measures the plausibility of factual triples with the form of $(\text{head entity}, \text{relation}, \text{tail entity})$ (or (h, r, t) in short), by processing the corresponding embedding vectors h, r, t .

A representative SF is TransE [8], which interprets the relation r as a translation from the head entity h to tail entity t . Variants of TransE project the entities to a relation-specific hyperplane to deal with relations involving 1-N/N-1/N-N mappings [17, 46, 54]. These models are categorized as translational distance models (TDMs). For another category, the bilinear models (BLMs) [26, 29, 33, 37, 38, 49, 56, 59], their SF can be regarded as using a bilinear product $h^\top R(r) t$ to model the interaction of entities and relations, where $R(r)$ is a square matrix related to relation embedding r . Inspired by the predictive performance of deep networks [6], the neural network

models (NNMs) have also been explored as scoring functions [12, 13, 21, 44, 50].

Concise model architectures make TDMs easy to be comprehended. However, they are shown to be less expressive and less effective [51, 53]. NNMs are more powerful but more expensive for training and prone to overfitting due to a large amount of parameters. In comparison, BLMs can express any KG under simple conditions by modeling relation of common properties (e.g., symmetric and anti-symmetric), and have achieved state-of-the-art performance [29]. Even though BLMs tend to be better than TDMs and NNMs for KG learning, there is currently no absolute winner among BLMs. We empirically observe that none of the existing scoring functions consistently perform the best in different datasets, and those better adapted for a certain KG dataset present better performance. Therefore, designing a model with fixed architecture that can adapt to different datasets is not the optimal solution.

Intuitively, one may raise the question: *can we design a specific scoring function for a given KG?* Usually, the scoring function is custom-designed by human experts in a trial-and-error way, which often requires much time and effort. To make the process of finding optimal SF more affordable and programmable, we need to bridge the gap between model design and the often scarce domain knowledge in KGE. Fortunately, the recently popular technique, automated machine learning (AutoML) comes into our sight.

AutoML has exhibited its great power in many machine learning tasks and applications [24, 57]. Inspired by AutoML and especially neural architecture search (NAS) techniques [15, 32, 62], we aim to design KG-dependent scoring functions. In this paper, we present an automated design method of scoring function, named AutoSF+. The proposed method can adapt to different KGs and different tasks, reducing human efforts in model design. However, it is not easy to achieve this goal, which requires domain knowledge in both areas of KGE and NAS. The preliminary work AutoSF [60] has designed a special greedy algorithm, enhanced with a filter and predictor to address the domain-specific properties of KGE, to design data-specific scoring functions. AutoSF is able to search better scoring functions on different datasets, however, the greedy algorithm usually leads to sub-optimal solutions [1, 48]. Hence, we improve AutoSF into AutoSF+ with the following three improvements:

- First, since the greedy algorithm cannot fully explore the search space and will lead to sub-optimal solutions, we improve it with the evolutionary algorithm, which is also enhanced by the filter and predictor.
- Second, we evaluate AutoSF+ on the recently developed benchmarks, i.e., ogbl-biokg and ogbl-wikikg2, which serve as a standard framework for graph learning and have larger scales than current benchmarks.

Table 1: Notations used in the paper.

$\mathcal{E}, \mathcal{R}, \mathcal{S}$	set of entities, relations, triples
$ \mathcal{E} , \mathcal{R} , \mathcal{S} $	number of entities, relations, triples
(h, r, t)	triple of head entity, relation and tail entity
$\mathbf{h}, \mathbf{r}, \mathbf{t}$	embeddings of h , r , and t
$f(h, r, t)$	scoring function for triple (h, r, t)
$\mathbb{R}^d, \mathbb{C}^d, \mathbb{H}^d$	d -dimensional real/complex/hypercomplex space
$\mathbf{R}(\mathbf{r}) \in \mathbb{R}^{d \times d}$	square matrix based on relation embedding \mathbf{r}
$\langle \mathbf{a}, \mathbf{b}, \mathbf{c} \rangle$	triple product := $\sum_{i=1}^d a_i b_i c_i = \mathbf{a}^\top \text{diag}(\mathbf{b}) \mathbf{c}$
$\ \mathbf{v}\ _1$	ℓ_1 -norm of vector \mathbf{v}
$\text{Re}(\mathbf{v})$	real part of complex vector $\mathbf{v} \in \mathbb{C}^d$
$\bar{\mathbf{v}}$	conjugate of complex vector $\mathbf{v} \in \mathbb{C}^d$

- Finally, we extend the application from KG completion to entity classification. By searching the message function in the GNN framework, we show that AutoSF+ can also improve the entity classification task.

Notations In this paper, vectors are denoted by lowercase boldface, and matrix by uppercase boldface. The commonly used notations are listed in Table 1.

2 RELATED WORKS

2.1 Knowledge Graph Embedding

A knowledge graph can be seen as a third-order tensor $\mathbf{G} \in \mathbb{R}^{|\mathcal{E}| \times |\mathcal{R}| \times |\mathcal{E}|}$. In this section, we consider embedding its entities and relations to a d -dimensional space. Let the resultant entity embedding matrix be $\mathbf{E} \in \mathbb{R}^{d \times |\mathcal{E}|}$ (with one column \mathbf{e} for each entity e) and the relation embedding matrix be $\mathbf{R} \in \mathbb{R}^{d \times |\mathcal{R}|}$ (with one column \mathbf{r} for each relation r). The *scoring function* $f(h, r, t) \in \mathbb{R}$ measures plausibility of the triple (h, r, t) based on the embeddings of h, r, t .

Algorithm 1 Training framework of knowledge graph embedding

Require: training triples \mathcal{S}_{tra} , scoring function f and loss function l .

- 1: initialize embeddings \mathbf{E} of entities and \mathbf{R} of relations.
- 2: **repeat**
- 3: sample a mini-batch $\mathcal{S}_{batch} \subset \mathcal{S}_{tra}$;
- 4: **for** each positive triple $(h, r, t) \in \mathcal{S}_{batch}$ **do**
- 5: sample negative triples $\tilde{\mathcal{S}}_{(h,r,t)} \equiv \{(h, r, \tilde{t})\}$ for (h, r, t) ;
- 6: compute loss l w.r.t. the score of triples in $\{(h, r, t)\} \cup \tilde{\mathcal{S}}_{(h,r,t)}$;
- 7: **end for**
- 8: update learnable parameters through backward propagation;
- 9: **until** convergence
- 10: **return** embeddings \mathbf{E} and \mathbf{R} .

KGE methods have been extensively studied in recent years. To obtain well-trained embeddings, most KGE models follow the learning procedure as in Algorithm 1. First, we initialize the embeddings of entities and relations in step 1 by Uniform or Xavier method [20]. For each positive triple in the training set, negative triples in step 5 are often sampled from fixed distribution [54] or dynamic schemes [46, 61]. Then, the hinge loss [8] and logistic loss [56] can be used as loss function l to maximize the score on positive triples and minimize the score on negative triples in step 6.

After that, the embeddings are updated based on stochastic gradient descent [27] in step 8.

The scoring function f , which is of central importance in the KGE task, can be examined from the two following aspects.

- *Expressiveness*. This considers the ability of the scoring function to fit a given KG.

Definition 2.1 (Expressiveness [4, 49, 52]). A SF f is *fully expressive* if for any KG G , there exists an entity embedding matrix \mathbf{E} and a relation embedding matrix \mathbf{R} such that $G_{hrt} = f(h, r, t), \forall h, t \in \mathcal{E}$ and $r \in \mathcal{R}$.

Among all the possible forms of KGs, there are special properties of relations. Common properties include symmetry, anti-symmetry, general asymmetry, and inverse. The fully expressive scoring functions can handle all the relation patterns.

- *Number of parameters*. Real-world KGs can be very sparse [45, 51]. A scoring function with a large number of trainable parameters may over-fit the training triples.

As mentioned in Section 1, current models mainly fall into three types: TDMs, BLMs and NNMs. It is well-known that many TDMs (such as TransE [8] and TransH [54]) cannot model the symmetric relations well [25, 51]. Neural network models, though fully expressive, have large numbers of parameters. This not only prevents the model from generalizing well on unobserved triples in a sparse KG, but also increases the training and inference costs [12, 29, 50]. In comparison, BLMs (except DistMult) can model all relation patterns and are fully expressive. Besides, these models usually have moderate complexities (with the number of parameters linear in $|\mathcal{E}|, |\mathcal{R}|$ and d). Therefore, we consider BLM as a better choice, and it will be our focus in this paper.

2.2 Neural Architecture Search

The automated machine learning (AutoML) [24, 57] has demonstrated its advantages in the design of better machine learning models. There are three important components in AutoML [5, 24, 57]: (i) *Search space*: This identifies important properties of the learning models to search. (ii) *Search algorithm*: A search algorithm is developed to search for good solutions in the designed space. (iii) *Evaluation*: Since the objective is to improve performance, evaluation is needed to offer feedbacks to the search algorithm.

The recent popularity of neural architecture search (NAS) has enabled the design of deep networks, such as CNN and RNN [15, 24, 62]. The search algorithms can be classified into two types, i.e. the model-based approach and the sample-based approach. Model-based approach builds a surrogate model for all candidates in the search space and uses the surrogate model to pick up candidates with promising performance, such as Bayesian algorithm [18], reinforcement learning algorithm [40, 62], and gradient-descent algorithm [32, 58]. The model-based approaches require evaluating a large number of architectures for training the surrogate model or require differentiable objective w.r.t. architectures. Sample-based approaches heuristically sample in the search space to explore better structures, such as greedy algorithm [31] and evolutionary algorithm [41]. The sample-based approaches are more flexible in selecting architectures and exploring the search space with strategies specific to a certain problem.

As for evaluation methods, parameter-sharing [32, 40, 58] allows faster architecture evaluation by combining architectures in the whole search space with the same set of parameters [5, 32, 40]. Despite the appealing speed, the obtained results can be sensitive to initialization, which hinders reproducibility [5]. On the other hand, stand-alone methods [3, 31, 41, 62] train and evaluate the different models separately. They are slower but more reliable. To improve the efficiency of stand-alone methods, a predictor can be trained to select promising architectures [31].

3 THE PROPOSED SEARCH PROBLEM

Real-world KGs are often large, sparse, incomplete as well as have distinct patterns, and it is unclear how a proper scoring function can be designed for a particular KG. In this section, we first provide a deep insight on current models, and then define "automated scoring function design" as a search problem based on the unified view of bilinear models.

3.1 Unifying Existing BLMs

Recall that a BLM may operate in the representation space that can be real, complex or hyper-complex. To present the different BLMs in the same form, we first unify them to the same representation space. The idea is to partition each of the embeddings $\mathbf{h}, \mathbf{r}, \mathbf{t}$ to 4 equal-sized chunks, i.e., $\mathbf{h} = [\mathbf{h}_1, \dots, \mathbf{h}_4], \mathbf{r} = [\mathbf{r}_1, \dots, \mathbf{r}_4]$ and $\mathbf{t} = [\mathbf{t}_1, \dots, \mathbf{t}_4]$. The BLM is then written in terms of $\{\langle \mathbf{h}_i, \mathbf{r}_j, \mathbf{t}_k \rangle\}_{i,j,k \in \{1, \dots, 4\}}$. In this way, current BLMs can be simplified and unified as follows.

- DistMult [56], which uses $f(\mathbf{h}, \mathbf{r}, \mathbf{t}) = \langle \mathbf{h}, \mathbf{r}, \mathbf{t} \rangle$. We simply split $\mathbf{h} \in \mathbb{R}^d$ (and analogously \mathbf{r} and \mathbf{t}) into 4 equal parts as $\{\mathbf{h}_1, \mathbf{h}_2, \mathbf{h}_3, \mathbf{h}_4\}$, where $\mathbf{h}_i \in \mathbb{R}^{d/4}$ for $i = 1, 2, 3, 4$. Obviously, $\langle \mathbf{h}, \mathbf{r}, \mathbf{t} \rangle = \langle \mathbf{h}_1, \mathbf{r}_1, \mathbf{t}_1 \rangle + \langle \mathbf{h}_2, \mathbf{r}_2, \mathbf{t}_2 \rangle + \langle \mathbf{h}_3, \mathbf{r}_3, \mathbf{t}_3 \rangle + \langle \mathbf{h}_4, \mathbf{r}_4, \mathbf{t}_4 \rangle$.
- Simple [26] / CP [29], which uses $f(\mathbf{h}, \mathbf{r}, \mathbf{t}) = \langle \hat{\mathbf{h}}, \hat{\mathbf{r}}, \hat{\mathbf{t}} \rangle + \langle \underline{\mathbf{t}}, \underline{\mathbf{r}}, \hat{\mathbf{h}} \rangle$. We split $\hat{\mathbf{h}} \in \mathbb{R}^d$ (and analogously $\hat{\mathbf{r}}$ and $\hat{\mathbf{t}}$) into 2 equal parts as $\{\mathbf{h}_1, \mathbf{h}_2\}$ (where $\mathbf{h}_1, \mathbf{h}_2 \in \mathbb{R}^{d/2}$), and similarly $\underline{\mathbf{h}}$ as $\{\mathbf{h}_3, \mathbf{h}_4\}$ (and analogously $\underline{\mathbf{r}}$ and $\underline{\mathbf{t}}$). Then, $\langle \hat{\mathbf{h}}, \hat{\mathbf{r}}, \hat{\mathbf{t}} \rangle + \langle \underline{\mathbf{t}}, \underline{\mathbf{r}}, \hat{\mathbf{h}} \rangle = \langle \mathbf{h}_1, \mathbf{r}_1, \mathbf{t}_3 \rangle + \langle \mathbf{h}_2, \mathbf{r}_2, \mathbf{t}_4 \rangle + \langle \mathbf{h}_3, \mathbf{r}_3, \mathbf{t}_1 \rangle + \langle \mathbf{h}_4, \mathbf{r}_4, \mathbf{t}_2 \rangle$.
- ComplEx [49] / HolE [37], which uses $f(\mathbf{h}, \mathbf{r}, \mathbf{t}) = \text{Re}(\mathbf{h} \otimes \mathbf{r} \otimes \bar{\mathbf{t}})$, where $\mathbf{h}, \mathbf{r}, \bar{\mathbf{t}}$ are complex-valued. Recall that any complex vector $\mathbf{v} \in \mathbb{C}^d$ is of the form $\mathbf{v}_r + i\mathbf{v}_i$, where $\mathbf{v}_r \in \mathbb{R}^d$ is the real part and $\mathbf{v}_i \in \mathbb{R}^d$ is the imaginary part. Thus,

$$\text{Re}(\mathbf{h} \otimes \mathbf{r} \otimes \bar{\mathbf{t}}) = \langle \mathbf{h}_r, \mathbf{r}_r, \mathbf{t}_r \rangle + \langle \mathbf{h}_i, \mathbf{r}_r, \mathbf{t}_i \rangle + \langle \mathbf{h}_r, \mathbf{r}_i, \mathbf{t}_i \rangle - \langle \mathbf{h}_i, \mathbf{r}_i, \mathbf{t}_r \rangle.$$

We split $\mathbf{h}_r \in \mathbb{R}^d$ (and analogously \mathbf{r}_r and \mathbf{t}_r) into 2 equal parts $\{\mathbf{h}_1, \mathbf{h}_2\}$ (where $\mathbf{h}_1, \mathbf{h}_2 \in \mathbb{R}^{d/2}$), and similarly $\mathbf{h}_i = \{\mathbf{h}_3, \mathbf{h}_4\}$ (and analogously \mathbf{r}_i and \mathbf{t}_i). Then,

$$\begin{aligned} \text{Re}(\mathbf{h} \otimes \mathbf{r} \otimes \bar{\mathbf{t}}) &= (\langle \mathbf{h}_1, \mathbf{r}_1, \mathbf{t}_1 \rangle + \langle \mathbf{h}_2, \mathbf{r}_2, \mathbf{t}_2 \rangle) + (\langle \mathbf{h}_3, \mathbf{r}_1, \mathbf{t}_3 \rangle + \langle \mathbf{h}_4, \mathbf{r}_2, \mathbf{t}_4 \rangle) \\ &\quad + (\langle \mathbf{h}_1, \mathbf{r}_3, \mathbf{t}_3 \rangle + \langle \mathbf{h}_2, \mathbf{r}_4, \mathbf{t}_4 \rangle) - (\langle \mathbf{h}_3, \mathbf{r}_3, \mathbf{t}_1 \rangle - \langle \mathbf{h}_4, \mathbf{r}_4, \mathbf{t}_2 \rangle). \end{aligned}$$

- Analogy [33], which uses $f(\mathbf{h}, \mathbf{r}, \mathbf{t}) = \langle \hat{\mathbf{h}}, \hat{\mathbf{r}}, \hat{\mathbf{t}} \rangle + \text{Re}(\underline{\mathbf{h}} \otimes \underline{\mathbf{r}} \otimes \bar{\mathbf{t}})$. We split $\hat{\mathbf{h}} \in \mathbb{R}^d$ (and analogously $\hat{\mathbf{r}}$ and $\hat{\mathbf{t}}$) into 2 equal parts $\{\mathbf{h}_1, \mathbf{h}_2\}$ (where $\mathbf{h}_1, \mathbf{h}_2 \in \mathbb{R}^{d/2}$), and similarly $\underline{\mathbf{h}} \in \mathbb{C}^{d/2}$ (and analogously $\underline{\mathbf{r}}$ and $\bar{\mathbf{t}}$) into 2 parts $\{\mathbf{h}_3, \mathbf{h}_4\}$ (where $\mathbf{h}_3, \mathbf{h}_4 \in \mathbb{R}^{d/2}$). Then,

$$\begin{aligned} \langle \hat{\mathbf{h}}, \hat{\mathbf{r}}, \hat{\mathbf{t}} \rangle + \text{Re}(\underline{\mathbf{h}} \otimes \underline{\mathbf{r}} \otimes \bar{\mathbf{t}}) &= \langle \mathbf{h}_1, \mathbf{r}_1, \mathbf{t}_1 \rangle + \langle \mathbf{h}_2, \mathbf{r}_2, \mathbf{t}_2 \rangle + \langle \mathbf{h}_3, \mathbf{r}_3, \mathbf{t}_3 \rangle \\ &\quad + \langle \mathbf{h}_3, \mathbf{r}_4, \mathbf{t}_4 \rangle + \langle \mathbf{h}_4, \mathbf{r}_3, \mathbf{t}_4 \rangle - \langle \mathbf{h}_4, \mathbf{r}_4, \mathbf{t}_3 \rangle. \end{aligned}$$

• QuatE [59], which uses $f(\mathbf{h}, \mathbf{r}, \mathbf{t}) = \mathbf{h} \odot \mathbf{r} \odot \mathbf{t}$. Recall that any hyper-complex vector $\mathbf{v} \in \mathbb{H}^d$ is of the form $\mathbf{v}_1 + i\mathbf{v}_2 + j\mathbf{v}_3 + k\mathbf{v}_4$, where $\mathbf{v}_1, \mathbf{v}_2, \mathbf{v}_3, \mathbf{v}_4 \in \mathbb{R}^d$. Thus,

$$\begin{aligned} \mathbf{h} \odot \mathbf{r} \odot \mathbf{t} &= \langle \mathbf{h}_1, \mathbf{r}_1, \mathbf{t}_1 \rangle - \langle \mathbf{h}_1, \mathbf{r}_2, \mathbf{t}_2 \rangle - \langle \mathbf{h}_1, \mathbf{r}_3, \mathbf{t}_3 \rangle - \langle \mathbf{h}_1, \mathbf{r}_4, \mathbf{t}_4 \rangle \\ &\quad + \langle \mathbf{h}_2, \mathbf{r}_2, \mathbf{t}_1 \rangle + \langle \mathbf{h}_2, \mathbf{r}_1, \mathbf{t}_2 \rangle + \langle \mathbf{h}_2, \mathbf{r}_4, \mathbf{t}_3 \rangle - \langle \mathbf{h}_2, \mathbf{r}_3, \mathbf{t}_4 \rangle \\ &\quad + \langle \mathbf{h}_3, \mathbf{r}_3, \mathbf{t}_1 \rangle - \langle \mathbf{h}_3, \mathbf{r}_4, \mathbf{t}_2 \rangle + \langle \mathbf{h}_3, \mathbf{r}_1, \mathbf{t}_3 \rangle + \langle \mathbf{h}_3, \mathbf{r}_2, \mathbf{t}_4 \rangle \\ &\quad + \langle \mathbf{h}_4, \mathbf{r}_4, \mathbf{t}_1 \rangle + \langle \mathbf{h}_4, \mathbf{r}_3, \mathbf{t}_2 \rangle - \langle \mathbf{h}_4, \mathbf{r}_2, \mathbf{t}_3 \rangle + \langle \mathbf{h}_4, \mathbf{r}_1, \mathbf{t}_4 \rangle. \end{aligned}$$

As $\langle \mathbf{h}_i, \mathbf{r}_k, \mathbf{t}_j \rangle = \mathbf{h}_i^\top \text{diag}(\mathbf{r}_k) \mathbf{t}_j$, the above BLMs can be written in the form of the following bilinear function

$$\mathbf{h}^\top \mathbf{R}(\mathbf{r}) \mathbf{t}, \quad (1)$$

where $\mathbf{h} = [\mathbf{h}_1^\top, \dots, \mathbf{h}_4^\top]^\top, \mathbf{t} = [\mathbf{t}_1^\top, \dots, \mathbf{t}_4^\top]^\top \in \mathbb{R}^d$, and $\mathbf{R}(\mathbf{r}) \in \mathbb{R}^{d \times d}$ is a matrix with 4×4 blocks, each block being either $0, \pm \text{diag}(\mathbf{r}_1), \dots$, or $\pm \text{diag}(\mathbf{r}_4)$. Figure 1 shows graphically the $\mathbf{R}(\mathbf{r})$ for above BLMs.

3.2 A Unified Representation of BLMs

Using the above unified form, design of BLM can be simplified to designing $\mathbf{R}(\mathbf{r})$ in (1). Hence, we define the unified representation of BLMs in definition 3.1.

Definition 3.1 (Unified Bilinear Model). Given a structure matrix

$$\mathbf{A} \in \{0, \pm 1, \dots, \pm K\}^{K \times K}, \quad (2)$$

the desired scoring function is of the form

$$f_{\mathbf{A}}(\mathbf{h}, \mathbf{r}, \mathbf{t}) = \sum_{i,j=1}^K \text{sign}(A_{ij}) \langle \mathbf{h}_i, \mathbf{r}_{|A_{ij}|}, \mathbf{t}_j \rangle. \quad (3)$$

This covers all the previous BLMs when $K = 4$. A graphical illustration is shown in Figure 2. Let $g_{\mathbf{K}}(\mathbf{A}, \mathbf{r})$ outputs a matrix with $K \times K$ blocks, with its (i, j) -th block:

$$[g_{\mathbf{K}}(\mathbf{A}, \mathbf{r})]_{ij} = \text{sign}(A_{ij}) \cdot \text{diag}(\mathbf{r}_{|A_{ij}|}). \quad (4)$$

We define $\mathbf{r}_0 \equiv 0$, and $\text{sign}(0) = 0$. The form in (3) can be written more compactly as

$$f_{\mathbf{A}}(\mathbf{h}, \mathbf{r}, \mathbf{t}) = \mathbf{h}^\top g_{\mathbf{K}}(\mathbf{A}, \mathbf{r}) \mathbf{t}. \quad (5)$$

3.3 Searching for BLMs

As introduced in Section 2.2, AutoML is powerful in designing data-dependent machine learning models [15, 24, 62]. Using the family of unified BLMs in Definition 3.1 as the search space \mathcal{A} for structure matrix \mathbf{A} , the search for a data-specific BLM can be formulated as the following AutoML problem.

Definition 3.2 (AutoSF+). Let $F(\mathbf{P}; \mathbf{A})$ be a KG embedding model (where \mathbf{P} includes the entity embedding matrix \mathbf{E} and relation embedding matrix \mathbf{R} , and \mathbf{A} is the structure matrix) and $M(F, \mathcal{S})$ be the performance of F on triples \mathcal{S} (the higher the better). The AutoSF+ problem is formulated as:

$$\mathbf{A}^* \in \text{Arg max}_{\mathbf{A} \in \mathcal{A}} M(F(\mathbf{P}^*; \mathbf{A}), \mathcal{S}_{\text{val}}) \quad (6)$$

$$\text{s.t. } \mathbf{P}^* = \arg \max_{\mathbf{P}} M(F(\mathbf{P}; \mathbf{A}), \mathcal{S}_{\text{tra}}), \quad (7)$$

where $\mathcal{A} = \{\mathbf{A} = [A_{ij}] \in \mathbb{R}^{K \times K} \mid A_{ij} \in \{0, \pm 1, \dots, \pm K\} \forall i, j = 1, \dots, K\}$ contains all the possible choices of \mathbf{A} , \mathcal{S}_{tra} is the training set, and \mathcal{S}_{val} is the validation set.

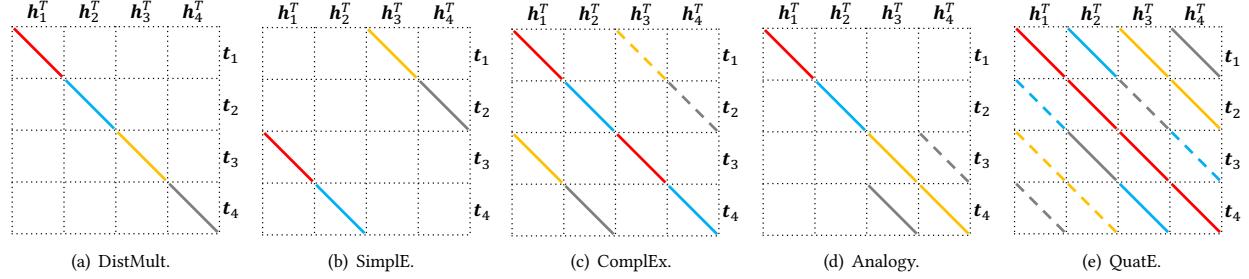


Figure 1: The forms of $R_{(r)}$ for representative BLMs (best viewed in color). Different colors correspond to different parts of $[r_1, r_2, r_3, r_4]$ (red for r_1 , blue for r_2 , yellow for r_3 , gray for r_4). Solid lines mean positive values, while dashed lines mean negative values. The empty parts have value zero.

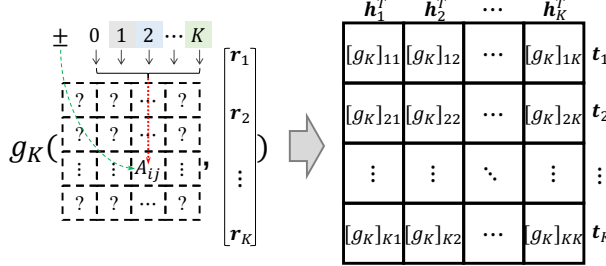


Figure 2: A graphical illustration of the form of $f_A(h, r, t)$.

Similar to the other AutoML problems [16, 18, 55, 62], AutoSF+ can be formulated as a bi-level optimization problem [10]. We first train the model to obtain P^* (converged model parameters) on the training set S_{tra} by (7), and then search for a better A (and consequently a better relation matrix $g_K(A, r)$) based on its performance M on the validation set S_{val} in (6). Note that the objectives in (6) and (7) are non-convex, and the search space is large (with $(2K+1)^{K^2}$ candidates). Thus, solving (7) can be expensive and challenging.

4 THE SEARCH ALGORITHM

In this section, we design efficient algorithms to search for the structure matrix A in (2). As in Section 2.2, model-based approaches require a proper surrogate model for the complex search space, or need a differentiable objective w.r.t. architectures on the non-differentiable ranking metrics. Both of them are impractical. Instead, we focus on the sample-based approaches. In Section 4.1, we introduce the properties specific to AutoSF+, which will then be addressed by the filter and predictor in Section 4.2. Finally, we present an evolutionary algorithm [55] (Section 4.3) that can be easily customized to work with the filter and predictor.

4.1 Properties Specific to Structure Matrices

In this part, we introduce two properties that are specific to the search space \mathcal{A} , and careful exploitation of these properties would be the key to success.

4.1.1 Degenerate Structures. Note that not all structure matrices A in (2) are equally good. For example, if all the nonzero blocks in $g_K(A, r)$ are in the first column, f_A will be zero for all head embeddings with $h_1 = 0$. We define degenerate structures that empirically perform bad and should be avoided.

Definition 4.1 (Degenerate structure). Matrix A is degenerate if (i) there exists $\mathbf{h} \neq 0$ such that $\mathbf{h}^\top g_K(A, \mathbf{r}) \mathbf{t} = 0, \forall \mathbf{r}, \mathbf{t}$; or (ii) there exists $\mathbf{r} \neq 0$ such that $\mathbf{h}^\top g_K(A, \mathbf{r}) \mathbf{t} = 0, \forall \mathbf{h}, \mathbf{t}$.

4.1.2 Equivalence. In general, two different A 's can have the same performance (as measured by M in Definition 3.2). This is captured in the following notion of equivalence. If a group of A 's are equivalent, we only need to evaluate one of them.

Definition 4.2 (Equivalence). Let $P^* = \arg \max_P M(F(P; A), \mathcal{S})$ and $P'^* = \arg \max_{P'} M(F(P'; A', \mathcal{S})$. If $A \neq A'$ but $M(F(P^*; A), \mathcal{S}) = M(F(P'^*; A'), \mathcal{S})$ for all \mathcal{S} , then A is equivalent to A' (denoted $A \equiv A'$).

4.2 Filter and Predictor

To search efficiently, one needs to (i) ensure that each new A is neither degenerate nor equivalent to an already-explored structure; and (ii) the scoring function $f_A(h, r, t)$ obtained from the new A is likely to have high performance. These can be achieved by designing an efficient filter (Section 4.2.1) and performance predictor (Section 4.2.2).

4.2.1 Filtering Degenerate and Equivalent Structures. The filtering procedure is shown in Algorithm 2. First, step 2 removes degenerate structure matrices. Next, step 3 generates a set of $(K!)^2 2^K$ structures that are equivalent to A . A is filtered out if any of its equivalent structures appear in the set \mathcal{H} containing structure matrices that have already been explored. As K is small, this filtering cost is very low compared with the cost of model training in (7).

Algorithm 2 Filtering degenerate and equivalent structure matrices.

Require: A : a $K \times K$ structure matrix, \mathcal{H} : a set of structures.

- 1: **initialization:** $Q(A, \mathcal{H}) = \text{True}$.
- 2: **if** $\det(A) = 0$ or $\{1, \dots, K\} \not\subset \{i, j \mid A_{ij} \neq 0, i, j = 1 \dots K\}$, **then**
 $Q(A, \mathcal{H}) = \text{False}$.
- 3: generate a set of equivalent structures $\{A' : A' \equiv A\}$ by enumerating permutation matrices P 's and sign vectors s 's.
- 4: **for** A' in $\{A' : A' \equiv A\}$ **do**
- 5: **if** $A' \in \mathcal{H}$, **then** $Q(A, \mathcal{H}) = \text{False}$, and exit the loop.
- 6: **end for**
- 7: **return** $Q(A, \mathcal{H})$.

4.2.2 Fast Evaluation with Predictor. After collecting N structures in \mathcal{H} , we construct a predictor \mathcal{P} to estimate the goodness of each \mathbf{A} . Note that search efficiency depends heavily on how to evaluate the candidate models. A highly efficient approach is parameter-sharing, as is popularly used in one-shot NAS [32, 40].

However, parameter sharing can be problematic when used to predict the performance $M(F(\mathbf{P}^*; \mathbf{A}), \mathcal{S}_{\text{val}})$ of scoring functions. Consider the two BLMs $f_{\mathbf{A}_1}(\mathbf{h}, \mathbf{r}, \mathbf{t}) = \langle \mathbf{h}, \mathbf{r}, \mathbf{t} \rangle$ and $f_{\mathbf{A}_2}(\mathbf{h}, \mathbf{r}, \mathbf{t}) = -\langle \mathbf{h}, \mathbf{r}, \mathbf{t} \rangle = -f_{\mathbf{A}_1}(\mathbf{h}, \mathbf{r}, \mathbf{t})$. When parameter sharing is used, it is likely that the predictor will output very different scores for the equivalent structures $\mathbf{A}_1 \equiv \mathbf{A}_2$. Hence, we train and evaluate the models separately as in the stand-alone evaluation [31, 55, 62].

Recall from Section 2.1 that it is desirable for the scoring function to be fully expressive. This motivates us to examine how many possible \mathbf{r} 's can lead to a symmetric or skew-symmetric $g_K(\mathbf{A}, \mathbf{r})$. To achieve this goal, we design symmetric-related features (SRF) with $K(K + 1)$ dimensions as the input for the predictor. Then, the predictor, a two-layer MLP, uses the SRF as input to predict the true performance. In this way, we can capture the symmetric related properties of different \mathbf{A} 's and then use the predictor to learn the correlation between SRF and empirical performance.

4.3 Evolutionary Algorithm

While the greedy search in AutoSF [60] can be efficient, however, some structures in the search space can never be explored and it will lead to sub-optimal solutions due to the limitation of the greedy algorithm [1, 48]. To address this problem, we consider the use of the evolutionary algorithm [2, 11].

Algorithm 3 shows the algorithm named AutoSF+. Same as AutoSF+, we start with structures with K non-zero elements. It initializes with a set \mathcal{I} of I non-degenerate and non-equivalent structures in step 1. Then, the main difference with the greedy algorithm in AutoSF [60] is in step 6 to step 11, where the new structures are generated by mutation and crossover. The mutation changes the value of each entry of a given structure \mathbf{A} to another value in $\{0, \pm 1, \dots, \pm K\}$ with a small probability p_m . As for crossover, given two structures $\mathbf{A}_{(a)}, \mathbf{A}_{(b)}$, each entry of the new structure has equal probabilities to be selected from the corresponding entries in either $\mathbf{A}_{(a)}$ or $\mathbf{A}_{(b)}$. After mutation and crossover, we check if the newly generated \mathbf{A}_{new} has to be filtered out. When N structures are collected, we use the predictor \mathcal{P} in Section 4.2.2 to select top- P structures. These are then trained and evaluated for performance. Finally, structures in \mathcal{I} with performance worse than the newly evaluated ones are replaced (step 14), i.e. the survive procedure. After repeating for several rounds until the budget is exhausted, the set \mathcal{I} , which stores I top-evaluated structures and returned.

5 EXPERIMENTS ON KG COMPLETION

We performed experiments to evaluate the proposed method on the knowledge graph completion (KGC) task. All algorithms are implemented in the pytorch [39] framework on a single RTX 2080Ti GPU (except some on RTX 8000 GPU with OGB dataset).

5.1 Setup

Knowledge graph completion (KGC) is a representative task in KG learning [8, 12, 26, 38, 49, 51, 56]. In this experiment, we use

Algorithm 3 Evolutionary search algorithm (AutoSF+).

Require: I, N, P : number of selected scoring functions by different components; K : the nonzero elements of structures in initial set. filter Q , and predictor \mathcal{P} .

- 1: **initialization:** initialize \mathcal{I} as a set of I non-degenerate and non-equivalent structures \mathbf{A} with K non-zero elements.
- 2: *train and evaluate* all \mathbf{A} 's in \mathcal{I} ;
- 3: add \mathbf{A} 's to \mathcal{T} and record the performance in \mathcal{Y} ;
- 4: **repeat**
- 5: update predictor \mathcal{P} with records in $(\mathcal{T}, \mathcal{Y})$.
- 6: **repeat**
- 7: $\mathcal{H} = \emptyset$;
- 8: **mutation:** sample $\mathbf{A} \in \mathcal{I}$ and mutate to get \mathbf{A}_{new} ; **or**
- 9: **crossover:** sample $\mathbf{A}_{(a)}, \mathbf{A}_{(b)} \in \mathcal{I}$ and crossover to get \mathbf{A}_{new} ;
- 10: if $Q(\mathbf{A}_{\text{new}}, \mathcal{H} \cup \mathcal{T})$ is true by Algorithm 2,
- 11: then $\mathcal{H} \leftarrow \mathcal{H} \cup \{\mathbf{A}_{\text{new}}\}$;
- 12: until $|\mathcal{H}| = N$;
- 13: select top- P structures \mathbf{A} in \mathcal{H} based on the the *predictor* \mathcal{P} ;
- 14: *train* embeddings and *evaluate* the performance of each \mathbf{A} ;
- 15: **survive:** update \mathcal{I} with \mathbf{A} if \mathbf{A} is better than the worst structure in \mathcal{I} ;
- 16: add \mathbf{A} 's in \mathcal{T} and record the performance in \mathcal{Y} ;
- 17: **until** budget is exhausted;
- 17: **return** \mathcal{I} .

the full multi-class log-loss [29], which is more robust and has better performance than negative sampling [29, 60]. As suggested by [29, 49], we use Adagrad [14] as the optimizer. Experiments are performed on five popular benchmark datasets: WN18, FB15k, WN18RR, FB15k237, YAGO3-10 and two newly developed datasets in the open graph benchmark (OGB) including ogbl-biokg and ogbl-wikikg2. Note that the OGB contains realistic and large-scale datasets, among which the ogbl-biokg dataset is relevant to both biomedical and fundamental ML research, while the ogbl-wikikg2 dataset captures the different types of relations between entities in the world. Statistics of these datasets are described in Table 2.

Table 2: Statistics of the KG completion datasets.

dataset	#entity	#relation	#train	#validate	#test
WN18 [8]	41k	18	141k	5k	5k
FB15k [8]	15k	1.3k	48k	50k	59k
WN18RR [12]	41k	11	87k	3k	3k
FB15k237 [47]	15k	237	272k	18k	20k
YAGO3-10 [35]	123k	37	1,079k	5k	5k
ogbl-biokg [23]	94k	51	4,763k	163k	163k
ogbl-wikikg2 [23]	2,500k	535	16,109k	429k	598k

Performance Measures: The learned scoring functions $f_{\mathbf{A}}(\mathbf{h}, \mathbf{r}, \mathbf{t})$ are evaluated in the context of link prediction. The following two metrics are computed by the ranks that are obtained after filtering all the other observed triples as in [8, 54]: (i) Mean reciprocal ranking (MRR): the average of the reciprocal of obtained ranks; and (ii) $H@k$: ratio of ranks no larger than k . The larger the MRR or $H@k$, the better is the scoring function.

Hyper-parameters: The search algorithms include the hyper-parameters $N = 128$, $P = 8$ and $I = 8$ in Algorithm 3. The mutation and crossover operations have equal probabilities. When the mutation is selected, the value of each entry has a mutation probability of $p_m = 2/K^2$. The budget (used to terminate the

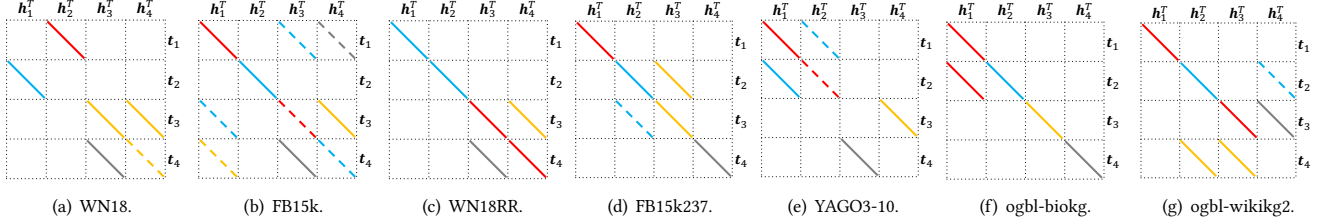


Figure 3: Graphical illustration of the BLMs obtained by AutoSF+ on the KG completion task. Different colors correspond to different parts of $[r_1, r_2, r_3, r_4]$ (red for r_1 , blue for r_2 , yellow for r_3 , gray for r_4). Solid lines mean positive values, while dashed lines mean negative values. The empty parts represent zeros.

Table 3: Results on KG completion. The best model is highlighted in bold and the second best is underlined. “–” means that results are not reported in those papers.

model	WN18			FB15k			WN18RR			FB15k237			YAGO3-10			
	MRR	H@1	H@10	MRR	H@1	H@10	MRR	H@1	H@10	MRR	H@1	H@10	MRR	H@1	H@10	
(TDM)	TransH	0.521	—	94.5	0.452	—	76.6	0.186	—	45.1	0.233	—	40.1	—	—	
	RotateE	—	—	—	0.797	74.6	88.4	0.476	42.8	<u>57.1</u>	0.338	24.1	53.3	0.488	39.6	66.3
	PairRE	—	—	—	0.811	76.5	89.6	—	—	—	0.351	25.6	54.4	—	—	—
(NNM)	Conve	0.942	93.5	95.5	0.745	67.0	87.3	0.46	39.	48.	0.316	23.9	49.1	0.52	45.	66.
	RSN	0.94	92.2	95.3	—	—	—	—	—	—	0.28	20.2	45.3	—	—	—
	CompGCN	—	—	—	—	—	—	0.479	44.3	54.6	0.355	26.4	53.5	—	—	—
(BLM)	TuckER	0.953	94.9	95.8	0.795	74.1	89.2	0.470	44.3	52.6	0.358	26.6	54.4	—	—	—
	DistMult	0.821	71.7	95.2	0.775	71.4	87.2	0.443	40.4	50.7	0.352	25.9	54.6	0.552	47.1	68.9
	SimplE/CP	0.950	94.5	<u>95.9</u>	0.826	79.4	90.1	0.462	42.4	55.1	0.350	26.0	54.4	0.565	49.1	71.0
	HoleE/ComplEx	0.951	94.5	95.7	0.831	79.6	90.5	0.471	43.0	55.1	0.345	25.3	54.1	0.563	49.0	70.7
	Analogy	0.950	94.6	95.7	0.816	78.0	89.8	0.467	42.9	55.4	0.348	25.6	54.7	0.557	48.5	70.4
	QuatE	0.950	94.5	95.9	0.782	71.1	90.0	0.488	43.8	58.2	0.348	24.8	55.0	0.556	47.4	70.4
AutoSF	<u>0.952</u>	<u>94.7</u>	96.1	<u>0.853</u>	<u>82.1</u>	<u>91.0</u>	<u>0.490</u>	<u>45.1</u>	56.7	<u>0.360</u>	<u>26.7</u>	<u>55.2</u>	<u>0.571</u>	<u>50.1</u>	71.5	
AutoSF+	<u>0.952</u>	<u>94.7</u>	96.1	<u>0.861</u>	<u>83.2</u>	<u>91.3</u>	0.492	<u>45.2</u>	56.7	<u>0.364</u>	<u>27.0</u>	<u>55.3</u>	<u>0.577</u>	<u>50.2</u>	71.5	

algorithm) is 256 structures on WN18, FB15k, WN18RR, FB15k-237, 128 on YAGO3-10, ogbl-biokg, and 64 on ogbl-wikikg. Note that the performance ranking of SFs is empirically consistent across different choices of dimension d . Hence, to reduce training time during searching, we set the dimension of the models to be $d = 64$.

After searching, the learning hyper-parameters on WN18, FB15k, WN18RR, FB15k237 and YAGO3-10 are selected from the following ranges: learning rate η in $[0, 1]$, ℓ_2 -penalty λ in $[10^{-5}, 10^{-1}]$, batch size m in $\{256, 512, 1024\}$, and dimension d in $\{256, 512, 1024, 2048\}$. For ogbl-biokg and ogbl-wikikg2, we follow the hyper-parameter settings in [46]. We use hyperopt [7] to search for the best hyper-parameter setting based on the validation set.

Baselines: AutoSF+ are compared with the following KG embedding models: (i) TDM: TransH [54], RotateE [46], and PairRE [9]; (ii) NNM: ConvE [12], RSN [21] and CompGCN [50]; (iii) BLM: TuckER [4], DistMult [56], SimplE [26], CP [29], HoleE [37], ComplEx [49], Analogy [33], QuatE [59] and AutoSF [60].

Table 4: Performance on ogbl-biokg dataset.

Model	Dim	Test MRR	Val MRR	#Params
PairRE	2000	0.8164 ± 0.0005	0.8172 ± 0.0005	187,750,000
ComplEx	2000	0.8095 ± 0.0007	0.8105 ± 0.0001	187,648,000
DistMult	2000	0.8043 ± 0.0003	0.8055 ± 0.0003	187,648,000
RotateE	2000	0.7989 ± 0.0004	0.7997 ± 0.0002	187,597,000
TransE	2000	0.7452 ± 0.0004	0.7456 ± 0.0003	187,648,000
AutoSF+	1000	0.8309 ± 0.0008	0.8317 ± 0.0007	93,824,000
AutoSF+	2000	0.8320 ± 0.0007	0.8327 ± 0.0006	187,648,000

Table 5: Performance on ogbl-wikikg2 dataset.

Model	Dim	Test MRR	Val MRR	#Params
PairRE	200	0.5208 ± 0.0027	0.5423 ± 0.0020	500,334,800
RotatE	250	0.4332 ± 0.0025	0.4353 ± 0.0028	1,250,435,750
TransE	500	0.4256 ± 0.0030	0.4272 ± 0.0030	1,250,569,500
ComplEx	250	0.4027 ± 0.0027	0.3759 ± 0.0016	1,250,569,500
ComplEx	50	0.3804 ± 0.0022	0.3534 ± 0.0052	250,113,900
DistMult	500	0.3729 ± 0.0045	0.3506 ± 0.0042	1,250,569,500
DistMult	100	0.3447 ± 0.0082	0.3150 ± 0.0088	250,113,900
TransE	100	0.2622 ± 0.0045	0.2465 ± 0.0020	250,113,900
RotatE	50	0.2530 ± 0.0034	0.2250 ± 0.0035	250,087,150
AutoSF+	100	0.5186 ± 0.0065	0.5239 ± 0.0074	250,113,900
AutoSF+	200	0.5458 ± 0.0052	0.5510 ± 0.0063	500,227,800

5.2 Performance

Table 3 shows the testing results for the five popular datasets, i.e., WN18, FB15k, WN18RR, FB15k237 and YAGO3-10. As can be seen, there is no clear winner among the baselines. For example, in terms of MRR, TuckER is the best among the baselines on WN18, but not good on FB15k. DistMult, though not fully expressive, is comparable with the other fully expressive BLMs on FB15k237, but inferior on the other datasets. CompGCN runs out of memory for larger KGs, e.g. WN18, FB15k, YAGO3-10, since the entire KG is used in each iteration. AutoSF performs consistently well. It outperforms the baselines on FB15k, WN18RR, FB15k237 and YAGO3-10, and is the first runner-up on WN18. AutoSF+ further improves AutoSF on FB15k, WN18RR, FB15k237 and YAGO3-10.

Comparisons on ogbl-biokg and ogbl-wikikg2 are shown in Table 4 and Table 5, respectively. AutoSF+ achieves state-of-the-art performances on the two OGB datasets: (i) for ogbl-biokg dataset, AutoSF+ out-performs other BLMs or TDMs, improving Test MRR nearly to 1.5% with only half of embedding dimension; (ii) on larger-scale dataset ogbl-wikikg2, AutoSF+ improves Test MRR close to 2.5% with the dimension of 200. These results further demonstrate the importance of searching scoring functions for learning embeddings. The searched scoring functions are shown in Figure 3. As can be seen, they are different from each other and are novel compared with the human-designed BLMs.

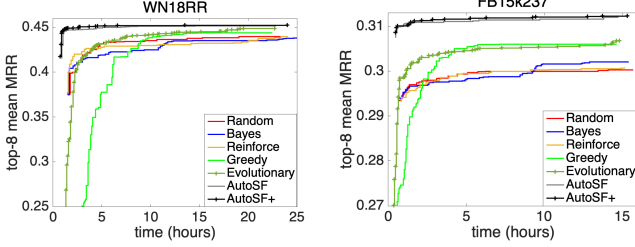


Figure 4: Comparison of different search algorithms.

5.3 Search Algorithm Comparison

In this experiment, we compared AutoSF+ with AutoSF [60] and the following search algorithms on the WN18RR and FB15k237 datasets.

- (i) Random, which samples each element of A independently and uniformly from $\{0, \pm 1, \dots, \pm K\}$;
- (ii) Bayes, which selects each element of A from $\{0, \pm 1, \dots, \pm K\}$ by performing hyperparameter optimization using the Tree Parzen estimator [7] and Gaussian mixture model (GMM);
- (iii) Reinforce, which generates the K^2 elements in A by using a LSTM [22] recurrently as in NAS-Net [62];
- (iv) Greedy, AutoSF without filter and predictor;
- (v) Evolutionary, AutoSF+ (Alg.3) without filter and predictor.

Figure 4 shows the mean validation MRR of the top $I = 8$ structures w.r.t. clock time. First, the Bayes and Reinforce algorithms do not show many advantages over the random search since their surrogate model cannot well address the properties in our search space. Second, Greedy and Evolutionary, even without filter and predictor, outperform the other search algorithms, showing the importance of gradually adjusting scoring functions during searching. AutoSF and AutoSF+ clearly outperform the others with the filter and predictor to deal with the domain-specific properties. Comparing with AutoSF, AutoSF+ is better since the evolutionary algorithm can explore the search space more flexibly.

6 EXTENSION TO ENTITY CLASSIFICATION

Entity classification aims at predicting the labels of the unlabeled entities. Since the labeled entities are few, a common approach is to use graph neural networks [19, 28] to aggregate the neighborhood information. Given the knowledge graph, representative works, including the R-GCN [44] and CompGCN [50], aggregate representations of all the entities layer-by-layer as:

$$\mathbf{e}_i^{\ell+1} = \sigma(\mathbf{e}_i^\ell + \sum_{(r,j):(i,r,j) \in S_{tra}} \phi(\mathbf{e}_j^\ell, \mathbf{r}^\ell)).$$

Here, $\phi(\mathbf{e}_j^\ell, \mathbf{r}^\ell)$ is a composition function that can significantly impact the performance [50] and S_{tra} contains all the training triples. R-GCN uses the composition operator in RESCAL [38], and defines $\phi(\mathbf{e}_j^\ell, \mathbf{r}^\ell) = R_{(r)}^\ell \mathbf{e}_j^\ell$, where $R_{(r)}$ is the relation specific weighting matrix in the ℓ -th layer. CompGCN, following TransE [8], DistMult [56] and Hole [37], defines three operators: subtraction $\phi(\mathbf{e}_j^\ell, \mathbf{r}^\ell) = \mathbf{W}^\ell(\mathbf{e}_j^\ell - \mathbf{r}^\ell)$, multiplication $\phi(\mathbf{e}_j^\ell, \mathbf{r}^\ell) = \mathbf{W}^\ell(\mathbf{e}_j^\ell \cdot \mathbf{r}^\ell)$ where \cdot is the element-wise product, and circular-correlation $\phi(\mathbf{e}_j^\ell, \mathbf{r}^\ell) = \mathbf{W}^\ell(\mathbf{e}_j^\ell \star \mathbf{r}^\ell)$, where $\mathbf{a} \star \mathbf{b} = \sum_{i=1}^d a_i b_{k+i-1 \bmod d}$. As mentioned in [50], the choice of composition function is important in learning embeddings. In this task, we use the following bilinear mapping for ϕ : $\phi(\mathbf{e}_u^\ell, \mathbf{r}^\ell) = g_K(\mathbf{A}, \mathbf{r}^\ell) \mathbf{e}_u^\ell$, to see whether the form of \mathbf{A} can benefit representations learning on the entire graph. The structure of \mathbf{A} is also searched under Definition 3.2, with 5-fold classification accuracy as performance measure.

6.1 Setup

Three datasets are used (Table 6): AIFB, which is an affiliation graph; MUTAG, which is a bioinformatics graph; and BGS, which is a geological graph. More details can be found in [43]. In these datasets, only a few entities have labels, and all the entities do not have attributes. Thus for the GCN-based methods, we use the entity's trainable embedding as input.

Table 6: Data sets used in entity classification.

dataset	#entity	#relation	#edges	#train	#test	#classes
AIFB	8,285	45	29,043	140	36	4
MUTAG	23,644	23	74,227	272	68	2
BGS	333,845	103	916,199	117	29	2

The following four models are compared: (i) GCN [28] without leveraging the relations of edges, i.e. $\phi(\mathbf{e}_j^\ell, \mathbf{r}^\ell) = \mathbf{W}^\ell \mathbf{e}_j^\ell$; (ii) R-GCN [44] with $\phi(\mathbf{e}_j^\ell, \mathbf{r}^\ell) = R_{(r)}^\ell \mathbf{e}_j^\ell$, with $R_{(r)}^\ell \in \mathbb{R}^{d \times d}$; (iii) CompGCN [50] with $\phi(\mathbf{e}_j^\ell, \mathbf{r}^\ell) = \mathbf{e}_j^\ell (-*/\star) \mathbf{r}^\ell$, in which the operator is chosen based on 5-fold cross-validation accuracy; and (iv) AutoSF+ which uses the searched structure \mathbf{A} to form the message function $\phi(\mathbf{e}_j^\ell, \mathbf{r}^\ell) = g_K(\mathbf{A}, \mathbf{r}^\ell) \mathbf{e}_j^\ell$ in GCN.

The setting of the search algorithms' hyper-parameters is the same as in Section 5.1. As for the learning hyper-parameters, we search the embedding dimension d from $\{12, 20, 32, 48\}$, learning rate from $[10^{-5}, 10^{-1}]$ with Adam as the optimizer [27]. For the GCN, the hidden layer size is the same as the embedding dimension, the dropout rate p_1 for GCN's input layer is from $[0, 0.5]$, the dropout rate p_2 for the intermediate layers is from $[0, 0.5]$. We search for 50 hyper-parameter settings for each dataset. Since there is no validation data, we use 5-fold cross-validation to measure the accuracy of training data and use the cross-validation accuracy to select the hyper-parameters in AutoSF+.

6.1.1 *Results.* We run and evaluate each model 5 times and report the accuracy and standard deviation in Table 7. With different composition operators, R-GCN and CompGCN perform differently in the three datasets. R-GCN is slightly better than CompGCN in AIFB but is worse in the other two sparser datasets. By searching the composition operators, AutoSF+ wins over the baseline methods with more proper messaging functions for a certain dataset.

Table 7: Results on entity classification task.

dataset	AIFB	MUTAG	BGS
GCN	86.67±2.33	68.83±2.18	73.79±3.08
R-GCN	92.78±2.48	74.12±2.67	82.97±0.47
CompGCN	90.6±0.2	85.3±1.2	84.14±1.89
AutoSF+	96.66±1.24	85.88±1.32	86.17±1.31

7 CONCLUSION

In this paper, we propose AutoSF+, an algorithm to automatically design scoring functions for knowledge graph embedding. As an extension of AutoSF, we use an evolutionary algorithm to search in such a space for more flexible exploration. Results on the five common datasets, the two newly developed OGB datasets, and the entity classification task show that the searched scoring functions outperform existing hand-designed ones. And the proposed evolutionary algorithm is more efficient than greedy search in AutoSF.

REFERENCES

- [1] F. Bach. 2013. Learning with Submodular Functions: A Convex Optimization Perspective. *Foundations and Trends in Machine Learning* 6, 2-3 (2013), 145–373.
- [2] T. Bäck. 1996. *Evolutionary algorithms in theory and practice: evolution strategies, evolutionary programming, genetic algorithms*. Oxford university press.
- [3] B. Baker, O. Gupta, N. Naik, and R. Raskar. 2017. Designing neural network architectures using reinforcement learning. In *ICLR*.
- [4] I. Balážević, C. Allen, and T. M Hospedales. 2019. TuckER: Tensor Factorization for Knowledge Graph Completion. In *EMNLP*.
- [5] G. Bender, P. Kindermann, B. Zoph, V. Vasudevan, and Q. Le. 2018. Understanding and simplifying one-shot architecture search. In *ICML*. 549–558.
- [6] Y. Bengio, A. Courville, and P. Vincent. 2013. Representation learning: A review and new perspectives. *TPAMI* 35, 8 (2013), 1798–1828.
- [7] J. S Bergstra, R. Bardenet, Y. Bengio, and B. Kégl. 2011. Algorithms for hyper-parameter optimization. In *NIPS*. 2546–2554.
- [8] A. Bordes, N. Usunier, A. Garcia-Duran, J. Weston, and O. Yakhnenko. 2013. Translating embeddings for modeling multi-relational data. In *NeurIPS*. 2787–2795.
- [9] L. Chao, J. He, T. Wang, and W. Chu. 2020. PairRE: Knowledge Graph Embeddings via Paired Relation Vectors. *arXiv preprint arXiv:2011.03798* (2020).
- [10] B. Colson, P. Marcotte, and G. Savard. 2007. An overview of bilevel optimization. *Annals of operations research* 153, 1 (2007), 235–256.
- [11] K. De Jong. 1988. Learning with genetic algorithms: An overview. *Machine Learning* 3, 2-3 (1988), 121–138.
- [12] T. Dettmers, P. Minerini, P. Stenetorp, and S. Riedel. 2017. Convolutional 2D knowledge graph embeddings. In *AAAI*.
- [13] X. Dong, E. Gabrilovich, G. Heitz, W. Horn, N. Lao, K. Murphy, T. Strohmann, S. Sun, and W. Zhang. 2014. Knowledge vault: A web-scale approach to probabilistic knowledge fusion. In *SIGKDD*. 601–610.
- [14] J. Duchi, E. Hazan, and Y. Singer. 2011. Adaptive subgradient methods for online learning and stochastic optimization. *JMLR* 12, Jul (2011), 2121–2159.
- [15] T. Elsken, Jan H. Metzen, and F. Hutter. 2019. Neural Architecture Search: A Survey. *JMLR* 20, 55 (2019), 1–21.
- [16] S. Falkner, A. Klein, and F. Hutter. 2018. BOHB: Robust and Efficient Hyperparameter Optimization at Scale. In *ICML*. 1436–1445.
- [17] M. Fan, Q. Zhou, E. Chang, and T. F. Zheng. 2014. Transition-based knowledge graph embedding with relational mapping properties. In *PACLIC*.
- [18] M. Feurer, A. Klein, J. Eggensperger, J. Springenberg, M. Blum, and F. Hutter. 2015. Efficient and robust automated machine learning. In *NeurIPS*. 2962–2970.
- [19] J. Gilmer, S. Schoenholz, P. Riley, O. Vinyals, and G. Dahl. 2017. Neural message passing for Quantum chemistry. In *ICML*. 1263–1272.
- [20] X. Glorot and Y. Bengio. 2010. Understanding the difficulty of training deep feedforward neural networks. In *Proceedings of the thirteenth international conference on artificial intelligence and statistics*. JMLR Workshop, 249–256.
- [21] L. Guo, Z. Sun, and W. Hu. 2019. Learning to Exploit Long-term Relational Dependencies in Knowledge Graphs. In *ICML*. 2505–2514.
- [22] S. Hochreiter and J. Schmidhuber. 1997. Long short-term memory. *Neural Computation* 9, 8 (1997), 1735–1780.
- [23] W. Hu, M. Fey, M. Zitnik, Y. Dong, H. Ren, B. Liu, M. Catasta, and J. Leskovec. 2020. Open graph benchmark: Datasets for machine learning on graphs. *arXiv preprint arXiv:2005.00687* (2020).
- [24] F. Hutter, L. Kotthoff, and J. Vanschoren (Eds.). 2018. *Automated Machine Learning: Methods, Systems, Challenges*. Springer.
- [25] S. Ji, S. Pan, E. Cambria, P. Marttinen, and P. Yu. 2020. *A survey on knowledge graphs: Representation, acquisition and applications*. Technical Report arXiv:2002.00388.
- [26] M. Kazemi and D. Poole. 2018. SimplE embedding for link prediction in knowledge graphs. In *NeurIPS*.
- [27] D. Kingma and J. Ba. 2014. Adam: A method for stochastic optimization. *arXiv preprint arXiv:1412.6980* (2014).
- [28] T. Kipf and M. Welling. 2016. Semi-supervised classification with graph convolutional networks. *arXiv preprint arXiv:1609.02907* (2016).
- [29] T. Lacroix, N. Usunier, and G. Obozinski. 2018. Canonical tensor decomposition for knowledge base completion. In *ICML*.
- [30] C. Liu, L. Li, X. Yao, and L. Tang. 2019. A Survey of Recommendation Algorithms Based on Knowledge Graph Embedding. In *CSEI*. 168–171.
- [31] C. Liu, B. Zoph, S. Jonathon, W. Hua, L. Li, F.-F. Li, A. Yuille, J. Huang, and K. Murphy. 2018. Progressive neural architecture search. In *ECCV*.
- [32] H. Liu, K. Simonyan, and Y. Yang. 2019. DARTS: Differentiable architecture search. In *ICLR*.
- [33] H. Liu, Y. Wu, and Y. Yang. 2017. Analogical inference for multi-relational embeddings. In *ICML*. 2168–2178.
- [34] D. Lukovnikov, A. Fischer, J. Lehmann, and S. Auer. 2017. Neural network-based question answering over knowledge graphs on word and character level. In *WWW*. 1211–1220.
- [35] F. Mahdisoltani, J. Biega, and F. M Suchanek. 2013. Yago3: A knowledge base from multilingual wikipedias. In *CIDR*.
- [36] M. Nickel, K. Murphy, V. Tresp, and E. Gabrilovich. 2016. A review of relational machine learning for knowledge graphs. *Proc. IEEE* 104, 1 (2016), 11–33.
- [37] M. Nickel, L. Rosasco, and T. Poggio. 2016. Holographic embeddings of knowledge graphs. In *AAAI*. 1955–1961.
- [38] M. Nickel, V. Tresp, and H. Kriegel. 2011. A three-way model for collective learning on multi-relational data. In *ICML*, Vol. 11. 809–816.
- [39] A. Paszke, S. Gross, S. Chintala, G. Chanan, E. Yang, et al. 2017. Automatic differentiation in PyTorch. In *ICLR*.
- [40] H. Pham, M. Guan, B. Zoph, Q. Le, and J. Dean. 2018. Efficient Neural Architecture Search via Parameters Sharing. In *ICML*. 4095–4104.
- [41] E. Real, A. Aggarwal, Y. Huang, and Q. Le. 2019. Regularized evolution for image classifier architecture search. In *AAAI*, Vol. 33. 4780–4789.
- [42] H. Ren, W. Hu, and J. Leskovec. 2020. Query2box: Reasoning over Knowledge Graphs in Vector Space Using Box Embeddings. In *ICLR*.
- [43] P. Ristoski and H. Paulheim. 2016. Rdf2vec: Rdf graph embeddings for data mining. In *International Semantic Web Conference*. Springer, 498–514.
- [44] M. Schlichtkrull, T. Kipf, P. Bloem, R. Van Den Berg, I. Titov, and M. Welling. 2018. Modeling relational data with graph convolutional networks. In *ESWC*. Springer, 593–607.
- [45] A. Singhal. 2012. Introducing the knowledge graph: Things, not strings. *Official Google blog* 5 (2012).
- [46] Z. Sun, Z. Deng, J. Nie, and J. Tang. 2019. Rotate: Knowledge graph embedding by relational rotation in complex space. In *ICLR*.
- [47] K. Toutanova and D. Chen. 2015. Observed versus latent features for knowledge base and text inference. In *Workshop on CVSMC*. 57–66.
- [48] J. A Tropp. 2014. Greed is good: Algorithmic results for sparse approximation. *TIT* 50, 10 (2004), 2231–2242.
- [49] T. Trouillon, C. Dance, E. Gaussier, J. Welbl, S. Riedel, and G. Bouchard. 2017. Knowledge graph completion via complex tensor factorization. *JMLR* 18, 1 (2017), 4735–4772.
- [50] S. Vashishth, S. Sanyal, V. Nitin, and P. Talukdar. 2020. Composition-based Multi-Relational Graph Convolutional Networks. In *ICLR*.
- [51] Q. Wang, Z. Mao, B. Wang, and L. Guo. 2017. Knowledge graph embedding: A survey of approaches and applications. *TKDE* 29, 12 (2017), 2724–2743.
- [52] Y. Wang, R. Gemulla, and H. Li. 2017. On multi-relational link prediction with bilinear models. In *AAAI*.
- [53] Y. Wang, D. Ruffinelli, S. Broscheit, and R. Gemulla. 2018. *On evaluating embedding models for knowledge base completion*. Technical Report. arXiv:1812.06410.
- [54] Z. Wang, J. Zhang, J. Feng, and Z. Chen. 2014. Knowledge graph embedding by translating on hyperplanes. In *AAAI*, Vol. 14. 1112–1119.
- [55] L. Xie and A. Yuille. 2017. Genetic CNN. In *ICCV*. 1388–1397.
- [56] B. Yang, W. Yih, X. He, J. Gao, and L. Deng. 2015. Embedding entities and relations for learning and inference in knowledge bases. In *ICLR*.
- [57] Q. Yao and M. Wang. 2018. *Taking human out of learning applications: A survey on automated machine learning*. Technical Report. Arxiv: 1810.13306.
- [58] Q. Yao, J. Xu, W. Tu, and Z. Zhu. 2020. Efficient neural architecture search via proximal iterations. In *AAAI*.
- [59] S. Zhang, Y. Tay, L. Yao, and Q. Liu. 2019. Quaternion Knowledge Graph Embedding. In *NeurIPS*.
- [60] Y. Zhang, Q. Yao, W. Dai, and L. Chen. 2020. AutoSF: Searching Scoring Functions for Knowledge Graph Embedding. In *ICDE*. 433–444.
- [61] Y. Zhang, Q. Yao, Y. Shao, and L. Chen. 2019. NSCaching: simple and efficient negative sampling for knowledge graph embedding. In *ICDE*. 614–625.
- [62] B. Zoph and Q. Le. 2017. Neural architecture search with reinforcement learning. In *ICLR*.